BBA - Molecular Basis of Disease 1866 (2020) 165964

Contents lists available at ScienceDirect

BBA - Molecular Basis of Disease

journal homepage: www.elsevier.com/locate/bbadis

P-cadherin induces *anoikis*-resistance of matrix-detached breast cancer cells by promoting pentose phosphate pathway and decreasing oxidative stress

Bárbara Sousa[a,b], Joana Pereira[a,b], Ricardo Marques[c], Luís F. Grilo[c], Susana P. Pereira[c], Vilma A. Sardão[c], Fernando Schmitt[a,b,d], Paulo J. Oliveira[c], Joana Paredes[a,b,d,*]

[a] i3S - Instituto de Investigação e Inovação em Saúde, Universidade do Porto, Portugal
[b] IPATIMUP - Institute of Molecular Pathology and Immunology, University of Porto, Rua Dr. Roberto Frias s/n, 4200-465 Porto, Portugal
[c] CNC - Center for Neuroscience and Cell Biology, University of Coimbra, UC Biotech, Biocant Park, Cantanhede, Portugal
[d] Medical Faculty of the University of Porto, Porto, Portugal

ARTICLE INFO

Keywords:
P-cadherin
Breast cancer
Oxidative stress
Antioxidant
Matrix-detached
anoikis-resistant

ABSTRACT

Successful metastatic spreading relies on cancer cells with stem-like properties, glycolytic metabolism and increased antioxidant protection, allowing them to escape *anoikis* and to survive in circulation. The expression of P-cadherin, a poor prognostic factor in breast cancer, is associated with hypoxic, glycolytic and acidosis biomarkers. In agreement, P-cadherin-enriched breast cancer cell populations presents a glycolytic and an acid-resistance phenotype.

Our aim was to evaluate whether P-cadherin expression controls the glycolytic and oxidative phosphorylation fluxes of matrix-detached breast cancer cells, acting as an antioxidant and enhancing their survival in anchorage-independent conditions. By using matrix-detached breast cancer cells, we concluded that P-cadherin increases glucose-6-phosphate dehydrogenase expression, up-regulating the carbon flux through the pentose phosphate pathway, while inhibiting pyruvate oxidation to acetyl-coA via pyruvate dehydrogenase kinase-4 (PDK-4) activation. Accordingly, P-cadherin expression conferred increased sensitivity to dichloroacetate (DCA), a PDK inhibitor. P-cadherin expression also regulates oxidative stress in matrix-detached breast cancer cells, through the control of antioxidant systems, such as catalase and superoxide dismutases (SOD)1 and 2, providing these cells with an increased resistance to doxorubicin-induced *anoikis*. Importantly, this association was validated in primary invasive breast carcinomas, where an enrichment of SOD2 was found in P-cadherin-overexpressing breast carcinomas.

In conclusion, we propose that P-cadherin up-regulates carbon flux through the pentose phosphate pathway and decreases oxidative stress in matrix-detached breast cancer cells. These metabolic remodeling and antioxidant roles of P-cadherin can promote the survival of breast cancer cells in circulation and in metastatic sites, being a possible player in breast cancer therapeutic resistance to pro-oxidant-based interventions.

1. Introduction

Distant metastases are the major cause of death in breast cancer patients. Tissue invasion, systemic dissemination and colonization of secondary sites can be initiated by significant alterations in cancer cell-cell adhesion, namely through the downregulation of E-cadherin or by the upregulation of P-cadherin expression levels [1,2].

We have previously contributed to understand the role of P-cadherin expression in breast cancer, establishing it as a putative molecular target in this disease. We demonstrated that the overexpression of this myoepithelial marker is significantly associated to a worse disease-free and overall survival for the patients, when evaluated in the primary tumor as well as on metastatic lymph nodes [3,4]. Moreover, we showed for the first time that P-cadherin overexpression promotes collective cell invasion, tumorigenesis, self-renewal potential and *anoikis*-resistance of breast cancer cells, as well as resistance to radiotherapy [5–7]. The molecular mechanisms involve activation of the heterodimer α6β4 integrin, which potentiates binding between cancer cells and extracellular matrix laminin [8]. Moreover, P-cadherin expression decreases the E-cadherin suppressive invasive function, by inducing the disruption of the cellular membrane E-cadherin/p120-catenin complex [9,10]. Both signals induce the phosphorylation of Src-

* Corresponding author at: Epithelial Interactions in Cancer Group, i3S - Instituto de Investigação e Inovação em Saúde, Universidade do Porto, Portugal.
E-mail addresses: bsousa@ipatimup.pt (B. Sousa), jspereira@ipatimup.pt (J. Pereira), vimarisa@ci.uc.pt (V.A. Sardão), fschmitt@ipatimup.pt (F. Schmitt), pauloliv@cnc.uc.pt (P.J. Oliveira), jparedes@ipatimup.pt (J. Paredes).

https://doi.org/10.1016/j.bbadis.2020.165964
Received 19 June 2020; Received in revised form 4 September 2020; Accepted 4 September 2020
Available online 10 September 2020

family tyrosine kinases and focal adhesion kinase (FAK), as well as the activation of Rac1 small GTPase [10,11], which have been already confirmed to be involved in cancer cell invasion, metastasis and in the process of epithelial to mesenchymal transition (EMT) [12–14].

More recently, we have also shown that P-cadherin expression in breast cancer cells is associated with hypoxic, glycolytic and acidosis markers. Also, cell populations enriched for P-cadherin are more likely to exhibit increased glycolysis and to survive to metabolic-driven alterations [15,16]. Thus, taking this into account, we hypothesized in this work that P-cadherin is involved in the dissemination of matrix-detached breast cancer cells by regulating their glycolytic flux and allowing them to survive in circulation, probably even during detrimental anti-cancer therapeutic conditions. In accordance, we show here for the first time that P-cadherin acts as a survival factor in *anoikis*-resistant and ECM-detached breast cancer cells, by activating the pentose-phosphate-pathway (PPP), by limiting reactive oxygen species (ROS), and by inducing the cellular antioxidant defenses. Thus, molecular strategies that inhibit P-cadherin-mediated survival in circulating breast cancer cells may have potential as a therapeutic approach.

2. Materials and methods

2.1. Cell Culture

Human breast cancer cell lines were obtained as follows: MCF-7/AZ was provided by Prof. Marc Mareel (Ghent University, Belgium) and BT-20 was obtained from American Type Culture Collection (HTB19, ATCC, Manassas, VA, USA). The MCF-7/AZ cell line was retrovirally transduced to stable encode EGFP (LZRS-IRES-EGFP plasmid, MCF-7/AZ.mock cell line) or both P-cadherin and EGFP (LZRS-P-cad-IRES-EGFP plasmid, MCF-7/AZ.P-cad cell line), as previously described [5]. Cells were routinely maintained at 37 °C, 5% CO_2, in the following media (Invitrogen, Paisley, UK): DMEM for BT-20 and 50% DMEM +50% HamF12 for MCF-7/AZ, supplemented with 10% heat-inactivated fetal bovine serum (FBS), 100 IU/mL penicillin and 100 mg/mL streptomycin (Invitrogen).

2.2. siRNA transfection

Gene silencing was performed in BT-20 cells using a validated siRNA, specific for *CDH3* (50 nM, Hs_CDH3_6), with the following target sequence 5' AAGCCTCTTACCTGCCGTAAA 3′, from Qiagen (Hilden, Germany). Transfections were carried out using Lipofectamine 2000 (Invitrogen), according to manufacturer's recommended procedures and as previously described [15]. A scrambled siRNA targeting sequence 5' AATTCTCCGAACGTGTCACGT 3′, with no homology to any gene, was used as a negative control (Qiagen). Gene inhibition was evaluated by western blot after 48 h of cell transfection.

2.3. Antibodies and compounds

The primary antibodies used in this study were: P-cadherin (clone 56, BD Transduction Biosciences, San Jose, CA, USA), p-PDH Ser293 (ab177461, AbCam, Cambridge, UK), tPDH (ab197956, Abcam), HSP70 (sc-7298, Santa Cruz Biotechnologies, Santa Cruz, CA, USA), PDK1 (4A11, Invitrogen), PDK3 (HPA0146583, Sigma-Aldrich, St. Quentin Fallavier, France), PDK4 (ab89295, AbCam), G6PD (HPA000247, Sigma-Aldrich), SOD1 (Cell Signaling Technology, Danvers, MA, USA), SOD2 (HPA001814, Sigma-Aldrich), HIF-1α (clone 54, BD Transduction Biosciences) and GLUT1 (ab15309, AbCam). Dichloroacetate (DCA) was obtained from Sigma-Aldrich, and dissolved in sterile H_2O. Doxorubicin, from AbCam, was dissolved in DMSO. The concentrations of DCA and Doxorubicin were determined based on the IC50 in monolayer MCF-7/AZ (Prof. Marc Mareel's lab) and BT-20 (HTB19, ATCC) cultures.

2.4. Mammosphere forming efficiency (MFE) assay

Breast cancer cells were enzymatically harvested and manually disaggregated to form a single-cell suspension and resuspended in cold PBS. Cells were plated at the density of 500cells/cm^2 in non-adherent culture conditions, in 6-well plates coated with 1.2% poly(2-hydroxyethylmethacrylate)/95% ethanol (Sigma-Aldrich) and allowed to grow for 5 days, in DMEM/F12 containing B27 supplement (Invitrogen), 500 ng/mL of hydrocortisone, 40 ng/mL insulin, 20 ng/mL EGF in a humidified incubator at 37 °C and 5% (*v*/v) CO2. MFE was calculated as the number of mammospheres (≥50 μm) formed divided by the number of cells plated [7].

2.5. Collection of matrix-detached and anoikis-resistant breast cancer cells

After 5 days in anchorage-independent conditions, mammospheres composed by matrix-detached and *anoikis*-resistant breast cancer cells, were directly used to perform protein extraction, as well as to measure GSH/GSSG levels and catalase activity. Alternatively, mammospheres were dissociated using trypsin and cultured in appropriate plates coated with poly-D-lysine (Sigma-Aldrich). Plates were then centrifuged at 1,200 rpm for 1 min, incubated for 1 h at 37 °C, and used for further assays, namely for Seahorse XF^{e}96 Extracellular Flux Analyzer and for ROS measurement.

2.6. Protein extraction and western blot analysis

Protein lysates were prepared from cells using catenin lysis buffer [1% (*v*/v) Triton X- 100 and 1% (v/v) NP-40 (Sigma-Aldrich) in PBS] supplemented with 1:7 protease inhibitor cocktail (Roche Diagnostics, Indianapolis, USA) and with 1:100 phosphatase inhibitor cocktail 3 (Sigma-Aldrich) for 10 min, at 4 °C. Cell lysates were mixed with a vortex and centrifuged at 14,000 rpm at 4 °C, during 10 min. Supernatants were collected and protein concentration was determined using the Bradford assay (Bio-Rad Protein Assay kit, Bio-Rad). Proteins were dissolved in sample buffer [Laemmli with 5% (*v*/v) 2-β-mercaptoethanol and 5% (v/v) bromophenol blue] and boiled for 10 min at 95 °C. Samples were separated by sodium dodecyl sulfate polyacrylamide gel electrophoresis (SDS-PAGE) and proteins were transferred into nitrocellulose membranes [Hybond enhanced chemiluminescence (ECL), Amersham, Little Chalfont, UK]. For immunostaining, membranes were blocked for 1 h with 5% (*w*/v) non-fat dry milk in PBS containing 0.5% (*v*/v) Tween20 and incubated overnight at 4 °C with the primary antibodies, diluted in milk buffer as follows: P-cadherin (1:500), p-PDH (1:2,000), tPDH (1:3,000), HSP70 (1:2,000), PDK1 (1:1,000), PDK3 (1:250), PDK4 (1:500 in 5% BSA), G6PD (1:250), SOD1 (1:2000) and SOD2 (1:2,500). After washed with PBS-Tween20, membranes were incubated with horseradish peroxidase (HRP)-conjugated anti-mouse or anti-rabbit secondary antibodies (Santa Cruz Biotechnologies), diluted 1:2,000 for 1 h. Proteins blotted in the membranes were then detected using Enhanced Chemiluminescence (ECL) reagent (Amersham) as a substrate. Quantity One software (Bio-Rad) was used for quantification of the differences in protein expression comparing with HSP70 expression.

2.7. XF extracellular flux analyses

Matrix-detached breast cancer cells derived from mammospheres were plated in Seahorse XF^{e}96 Cell Culture microplates (Agilent, Santa Clara, CA, USA), previously coated with poly-D-lysine and collagen, at a cell density of 30,000 and 20,000 cells/well for MCF-7/AZ and BT-20 cells, respectively. After centrifugation, cells were incubated with mammosphere medium for 1 h at 37 °C. Oxygen consumption rates (OCR) measurements and the extracellular acidification rate (ECAR) were determined using a Seahorse XFe96 analyzer (Agilent). For the XF Cell Mito Stress kit (Agilent), the plate was washed with basal medium

containing 25 mM glucose, 0.5 mM pyruvate and 2.5 mM glutamine and incubated for 1 h at 37 °C. OCR and ECAR measurements were obtained in different respiratory states by sequential injection of 3 μM oligomycin, 0.5 μM FCCP and 1 μM rotenone/antimycin. For the glycolytic rate assay kit (Agilent), the experimental procedure was performed as previously described, except for the addition of 5 mM HEPES to base medium, and ECAR and OCR measurements were obtained by injection of 1 μM rotenone/antimycin and 50 mM 2-DG. Energy maps were built by using the OCR and ECAR values under basal conditions and following induced stress post-oligomycin and FCCP injection. Raw data were normalized to cell mass determined by the Sulforhodamine B (SRB) method [17], the results were analyzed using the Software Version Wave Desktop 2.6 and exported using the respective XF Report Generators (Agilent). OCR and ECAR values were used to calculate the glycolytic parameters and expressed as Glycolytic Proton Efflux Rate (GlycoPER) and PER (Proton Efflux Rate), accordingly to manufacturer guide.

2.8. Reactive oxygen species (ROS) assay

Matrix-detached and *anoikis*-resistant breast cancer cells obtained after 5 days growing in anchorage-independent conditions were plated in black 96 well plates with clear bottom. Cells were washed with PBS and DCFDA (Sigma-Aldrich) was added to a final concentration of 10 μM for 30 min at 37 °C, according to manufacturer's instructions. After washing twice, 200 μL of PBS was added to each well and fluorescence was read on λex = 485 nm and λem = 535 nm. DCFDA values were normalized to cell mass determined by the SRB assay [17].

2.9. Cell viability assay

Cells were plated in a 96-wells plate and allowed to grow overnight. DOX was added and incubated during 48 h. In the end of the treatment, cells were washed with PBS 1 × (phosphate buffered saline) and Presto Blue reagent (Invitrogen) was added at 1:20 diluted in culture medium. Cells were incubated at 37° C, 5% CO2 for 30 min and the fluorescence was read at 50% sensitivity top reading on the following wave-length (λ): λ excitation = 560 nm and λ emission = 590 nm.

2.10. Intracellular glutathione levels

Total glutathione content was determined by the glutathione reductase enzymatic method [18]. Briefly, matrix-detached breast cancer cells were lysed with 0.1% (*v*/v) Triton X-100, 0.6% 5-sulfosalicylic acid in assay buffer, and disrupted by sonication. Cell extracts were centrifuged at 3,000 *g* at 4 °C for 5 min. Supernatants were then used for quantification of total glutathione and oxidized glutathione (GSSG) levels alone (pre-incubation with 2-vinyl-pyridine for 1 h at room temperature and followed by triethanolamine for 10 min). Glutathione standards were run simultaneously with the samples. Reaction was initiated by adding 120 μL of working solution (5,5′-dithiobis 2-nitrobenzoic acid and glutathione reductase) with 20 μL of cell extract (20 μg protein) or 20 μL of glutathione standards. Next, 60 μL of 0.8 mM NADPH solution was added and the increase in absorbance was recorded at 412 nm wavelength for 2 min. Glutathione values obtained from standard curve were expressed as nmol/mg protein.

2.11. Catalase enzymatic determination

Catalase measurement was determined by adding hydrogen peroxide to the samples and following its decomposition over time at 240 nm described by Aebi [19] and adapted to microplates. After being collected, cell pellets were resuspended in 50 mM phosphate buffer solution (KH_2PO_4, $Na_2HPO_4{\cdot}H_20$, pH 7.8) and samples sonicated in ice. One hundred microgram of protein per each assay, done in duplicate, was prepared in phosphate buffer. The kinetic assay was initiated by adding 100 μL H_2O_2 (93 mM) to the microplate wells. The decrease in absorbance was monitored every 15 s for 2 min and half. Positive (pure catalase) and negative controls (sodium azide) were run simultaneously with the assay for method validation. Data analysis of the kinetic assay was performed by applying an exponential regression (one phase decay equation) of the linear part of the kinetic using GraphPad Prism 8 (GraphPad, Irvine, CA, USA). From the equation, data points in the first 15 s were obtained and a linear regression of them was performed. The slope was taken which corresponds to catalase maximal activity. Results were then expressed as fold-change relatively to control group.

2.12. Human breast tumor samples

Breast cancer samples were included in Tissue Microarays (TMAs) representing a series of 466 formalin-fixed, paraffin-embedded human invasive breast carcinomas, retrieved from the Department of Pathology, Hospital Xeral Cíes, Vigo, Spain, diagnosed between 1978 and 1992. Detailed information about clinical, pathological and molecular characteristics is described in Vieira et al. [7]. Since clinicopathological information was unavailable for some samples, as well as the immunohistochemical results was not interpretable for some markers, the statistical analyses were performed using only the breast tumor cases with available data for each variable. A complete description of the number and frequencies of all variables included in this study is summarized in Supplementary Table 1. The studies using this material were performed under national laws for the handling of biological specimens from tumor banks, being the samples exclusively available for research purposes in retrospective studies.

2.13. Immunohistochemistry

The immunohistochemical assays were performed with specific antibodies for SOD1 (1:50) and SOD2 (1:1,000). Standard immunohistochemistry protocol was used as previously described [20]. Epitope retrieval was achieved using high temperature (98 °C) in citrate buffer, followed by primary antibody incubation for 1 h at room temperature. The primary antibodies were detected using a secondary antibody with horse-radish peroxidase polymer (Cytomation Envision System HRP; DAKO Cytomation, Carpinteria, USA) and diamino-benzidine as chromogen, according to the manufacturer's instructions. Reactions were blinded evaluated by a breast cancer pathologist and scored semi-quantitatively for cytoplasmic staining as follows: 0: 0% of immunoreactive cells; 1: < 5% of immunoreactive cells; 2: 5–50% of immunoreactive cells; and 3: > 50% of immunoreactive cells. Intensity of staining was also scored semi-qualitatively as follows: 0: negative; 1: weak; 2: intermediate; and 3: strong. The final score was defined as the sum of both parameters (extension and intensity), and grouped as negative (score 0–2) and positive (score 3–6). Representative images of SOD1 and SOD2 immunohistochemistry score using this criteria are shown Supplementary Fig. 1.

Details concerning the immunohistochemistry protocol for P-cadherin, E-cadherin, the molecular markers ER, PR, HER2, CK5, CK14, EGFR, and Vimentin, the breast cancer stem cell markers CD44, CD24, ALDH1 and CD49f, and the hypoxia and glycolytic markers HIF-1α, GLUT1 and CAIX, as well as for all sample clinicopathological data, are described elsewhere [7,15,21].

Double immunohistochemistry for P-cadherin and HIF-1α was performed as previously described [22], using the Envision G2 Doublestain (Dako Cytomation), according to manufacturer's instructions. In double immunofluorescence for P-cadherin and GLUT1, performed as previously described [11,15], after overnight primary antibodies incubation, tissues were incubated for 1 h at room temperature with conjugated goat anti-mouse/rabbit secondary IgG diluted 1:500, (Dako Cytomation), respectively. After PBS washing, samples were mounted with Vectashield (Vector Laboratories, Inc., Burlingame, USA) containing 4,6-diamidine-2-phenylindolendihydro-chrolide (DAPI) and

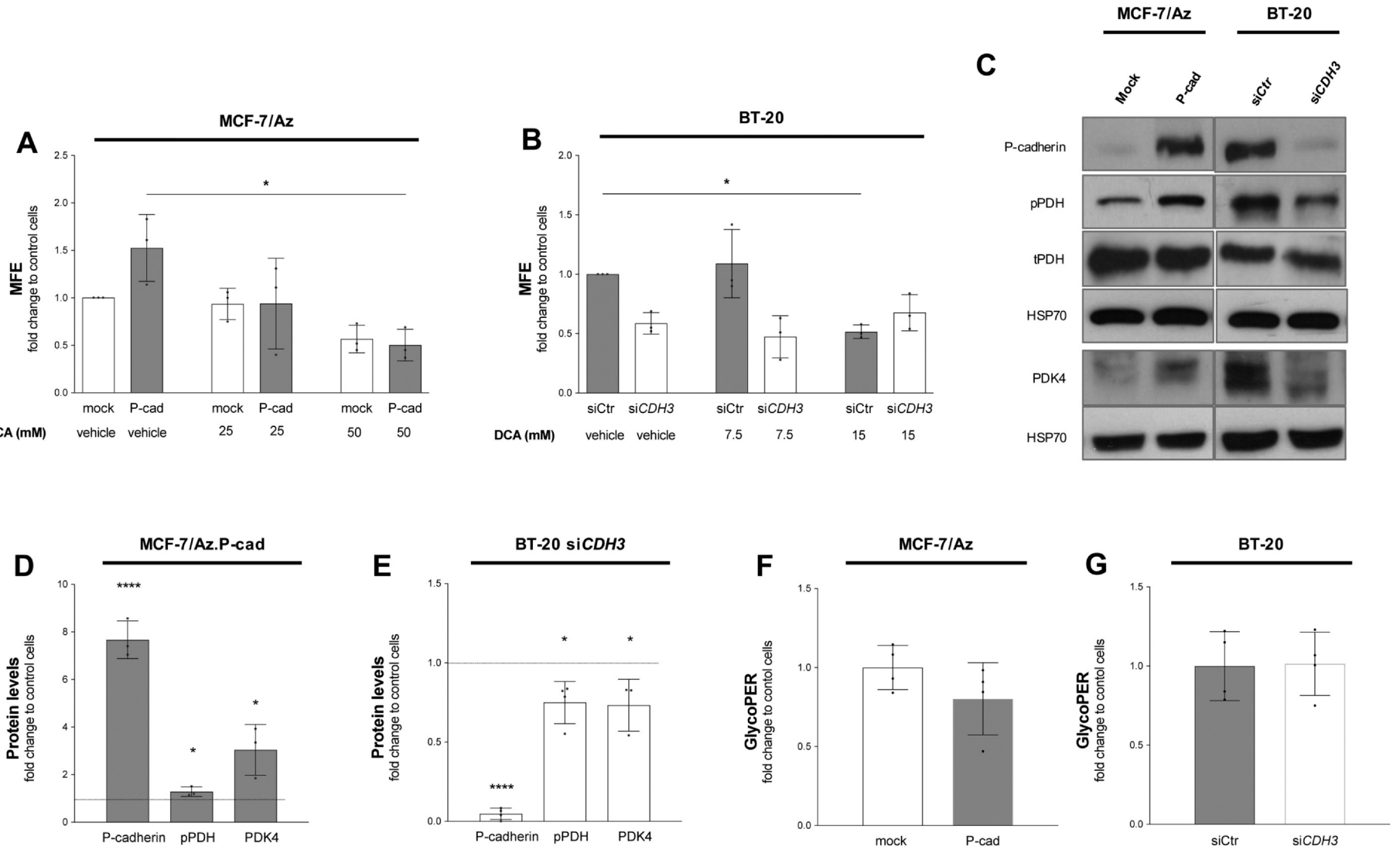

Fig. 1. Matrix-detached P-cadherin-enriched breast cancer cells are more sensitive to DCA-induced *anoikis* and present increased levels of PDK4-induced PDH phosphorylation. Under anchorage-independent conditions, P-cadherin overexpression induces an increased MFE in MCF-7/AZ cells (A). 25 and 50 mM DCA induces a decrease in MFE, either in MCF-7/AZ.mock and MCF-7/AZ.P-cad cells, being the effect stronger and statistically significant in breast cancer cells with increased P-cadherin expression treated with 50 mM of DCA ($p = 0.0308$) (A). In BT-20 model, *CDH3* silencing decreases MFE (B). Moreover, 7.5 mM of DCA showed no alterations in MFE in both control and *CDH3*-silenced cells, while 15 mM of DCA induced a statistically significant decrease in MFE in BT-20 siCtr cells ($p = 0.0372$), while no effect was observed in BT-20 si*CDH3* cells; (Mean ± SD, $N = 3$, $n \geq 3$, One-way ANOVA unpaired test). Representative image of western blot (C) of both MCF-7/AZ and BT-20 cell models and the quantification (D and E, respectively), shows that P-cadherin overexpression increases Ser293 phosphorylation of PDH ($p = 0.0286$) induced by PDK4 overexpression ($p = 0.0286$), while *CDH3* silencing decreases PDK4-induced pPDH ($p = 0.0286$); pPDH levels are normalized to total amount of PDH (Mean ± SD, $N \geq 3$, unpaired Mann-Whitney test). Basal Glycolysis was evaluated in both models (F and G), measured by the glycoPER (Glycolytic Proton Efflux Rate). In MCF-7/AZ cells, basal glycolysis is slightly decreased in P-cadherin-overexpressing cells, although not statistically different (F). No alterations are observed in BT-20 cells (G); data obtained was analyzed using Seahorse Data Analysis Software Wave Desktop 2.6 and the respective XF Stress Test Report Generator, and measured in pmol/min/cell mass; (Mean ± SD, $N = 3$–4, $n \geq 3$, unpaired Mann-Whitney test); (*$p < 0.0332$, **$p < 0.0021$ ***$p < 0.0002$, ****$p < 0.0001$).

visualized with Leica DM 2000 microscope (Leica Microsystems, Wetzlar, Germany).

2.14. Statistical analysis

Results are presented as the Mean ± SD of three or more independent biological repeats, each one with three or more technical replicates. Statistical analyses were performed using GraphPad Prism v8 software. Significance of difference was analyzed by one-way ANOVA with Kruskal–Wallis test followed by Dunn's multiple comparison test, or unpaired Mann-Whitney test, when appropriate. A p-value of < 0.05 was considered statistically significant. For immunohistochemistry in human breast carcinomas, $\chi 2$ test and contingency tables were used to determine associations between groups and the results were considered statistically significant when the p-value was lower than 0.05, using SPSS statistics 17.0 software (SPSS Inc., Chicago, USA).

3. Results

3.1. P-cadherin overexpression in matrix-detached breast cancer cells promotes higher susceptibility to DCA and increased PDK4-mediated PDH phosphorylation

In order to functionally evaluate whether P-cadherin-induced signaling can regulate the metabolic program of matrix-detached breast cancer cells, we evaluated the response of P-cadherin-enriched cells to DCA. Mechanistically, DCA targets glycolytic cells, inhibiting pyruvate dehydrogenase kinase (PDK), activating pyruvate dehydrogenase (PDH), and thus shifting cellular metabolism to oxidative phosphorylation [23]. This forced metabolism transition can trigger cell death in glycolytic tumors [23]. We used a previously described breast cancer model [3,15] in which P-cadherin was retrovirally transduced in MCF-7/AZ cells (MCF-7/AZ.P-cad, and the respective control MCF-7/AZ.-mock), and a second model in which P-cadherin was transiently silenced in BT-20 breast cancer cells, using a specific siRNA for *CDH3* (si*CDH3* vs siCtr). Cells were then treated with DCA for 24 h and plated in non-adherent conditions for 5 days, promoting the survival of *anoikis*-resistant breast cancer cells and the ability to form mammospheres, the MFE (Fig. 1A and B). As expected, the overexpression of P-cadherin promoted *anoikis*-resistance in vehicle-treated MCF-7/AZ cells, leading to a 53% increase of MFE (Fig. 1A). DCA treatment of MCF-7/AZ cells induced a dose-dependent effect in MFE (Fig. 1A). Specifically, 25 mM and 50 mM of DCA induced a 6% and 43% decrease in MFE, respectively, in MCF-7/AZ.mock cells, and a 38% and 67% decrease, respectively, in MCF-7/AZ.P-cadherin-overexpressing cells, being this effect stronger and statistically significant only in MCF-7/AZ.P-cad cell line treated with 50 mM of DCA ($p = 0.0308$) (Fig. 1A). Accordingly, in P-cadherin-overexpressing BT-20 breast cancer cells, a 41% decrease in MFE was also observed when P-cadherin was silenced with transient siRNA (BT-20 si*CDH3)* (Fig. 1B). Consistently, 7.5 mM of DCA showed no alterations in MFE in both control and P-cadherin-silenced cells, while 15 mM DCA induced a significant 48% decrease in MFE in P-cadherin-enriched BT-20 siCtr cells ($p = 0.0372$), but no significant alterations were observed in P-cadherin-silenced BT-20 cells (BT-20 si*CDH3*) when treated with DCA (Fig. 1B). These results demonstrate that matrix-detached P-cadherin-enriched breast cancer cells are *anoikis*-resistant, being more sensitive to DCA, in comparison to breast cancer cells with lower levels of P-cadherin. For this reason, we hypothesized that P-cadherin can actively signal to up-regulate the glycolytic flux. We next analyzed the total and phosphorylated PDH, the major metabolic checkpoint responsible for the rate-limiting step of pyruvate conversion to acetyl-CoA, determining also the flux towards lactate formation (Fig. 1C, D and E). We found that P-cadherin-overexpressing cells presented a 29% increase in Ser293 phosphorylation of PDH ($p = 0.0286$), the inactive form of PDH, preventing the conversion of pyruvate to acetyl-CoA and its entry into the Krebs cycle (Fig. 1C and D). In accordance, *CDH3*-silenced BT-20 breast cancer cells showed a 25% decreased pPDH/PDH when compared to control cells ($p = 0.0286$) (Fig. 1C and E). Since DCA modulates the glycolytic flux through PDK activation, we tested if P-cadherin expression would regulate PDK expression (Fig. 1C, D, E and Supplementary Fig. 2). Interestingly, P-cadherin overexpression in MCF-7/AZ breast cancer cells led to a two-fold increase of PDK4 expression ($p = 0.0286$) (Fig. 1C and D); in BT-20 cells, P-cadherin silencing also induced a 27% decrease in PDK4 levels ($p = 0.0286$) in comparison to control BT-20 cells (Fig. 1C and E). No alterations were found in other PDK isoforms, such as PDK1 and PDK3 (Supplementary Fig. 2), except for a 29% increase in PDK1 upon *CDH3* silencing in BT-20 cells ($p = 0.0286$).

We next used the Seahorse XF^{e}96 Extracellular Flux Analyzer (Seahorse Bioscience) to evaluate the effect of P-cadherin expression in the OCR and ECAR of matrix-detached breast cancer cells. Interestingly, despite the previous results, we did not observe any statistically significant alteration in any parameter evaluated (Fig. 1F, G and Fig. Supplementary Fig. 3). However, P-cadherin-enriched MCF-7/AZ cells showed a 20% decrease in media acidification related with basal glycolysis (Fig. 1F). Although the difference was not statistically significant, this effect suggests a small, but consistent, decrease in extracellular lactate; the same effect was not observed in BT-20 model (Fig. 1G). Additionally, the contribution of the proton leak and ATP-associated OCR for basal respiration was found slightly increased (by 17%) and decreased (by 7%), respectively, in *CDH3*-silenced BT-20 cells, while the contributions were unchanged in MCF-7/AZ cells (Fig. Supplementary Fig. 3).

We next performed energy maps using the Seahorse data in unstressed and stressed cells (Supplementary Fig. 4). Under stress conditions, P-cadherin overexpression in MCF-7/AZ breast cancer cells showed increased reliance on glycolytic metabolism comparatively to control cells. The effect was less obvious in BT20 cells.

Thus, these results suggested that P-cadherin-enriched cells present a higher reliance on the glycolytic metabolism, being more sensitive to DCA, with an increased PDK4-induced PDH phosphorylation, as well as a slight decrease in media acidification relative to basal glycolysis.

3.2. P-cadherin expression up-regulates G6PD and attenuates the oxidative stress of matrix-detached breast cancer cells

One possibility for the data obtained so far in MCF-7/AZ cells is that P-cadherin expression could be deviating the metabolic flux into the oxidative arm of the pentose phosphate pathway (PPP), which is involved with the up-regulation of antioxidant capacity via NADPH production. To demonstrate this, we next evaluated the expression of G6PD, a rate-limiting PPP enzyme (Fig. 2A and B). We found that matrix-detached P-cadherin-enriched MCF-7/AZ breast cancer cells presented a 41% increased G6PD protein content in comparison to control MCF-7/AZ.mock cells ($p = 0.0286$) (Fig. 2A and B). However, no significant differences were found in BT-20 cells (Fig. 2A and B).

Since PPP is the major source of NADPH, required not only for biosynthesis but also to support antioxidant GSH activity, which potentiates an undifferentiated cell phenotype and inhibition of *anoikis* [24], we next evaluated whether P-cadherin expression could be implicated in the regulation of cellular ROS. For that, we have used the DCFDA fluorescent dye in detached breast cancer cells, using tBHP as a positive control (Fig. 2C and D). Matrix-detached P-cadherin-overexpressing MCF-7/AZ breast cancer cells showed a statistically significant 33% decrease of intracellular oxidative stress ($p = 0.0286$), in comparison to MCF-7/AZ.mock cells (Fig. 2C). Accordingly, we observed a 48% increase in cellular oxidative stress in BT-20 after *CDH3* silencing (Fig. 2D), although this difference was not statistically significant due to data scattering.

Since increased cellular oxidative stress promotes sensitivity to chemo and radiotherapy, we further evaluated whether P-cadherin

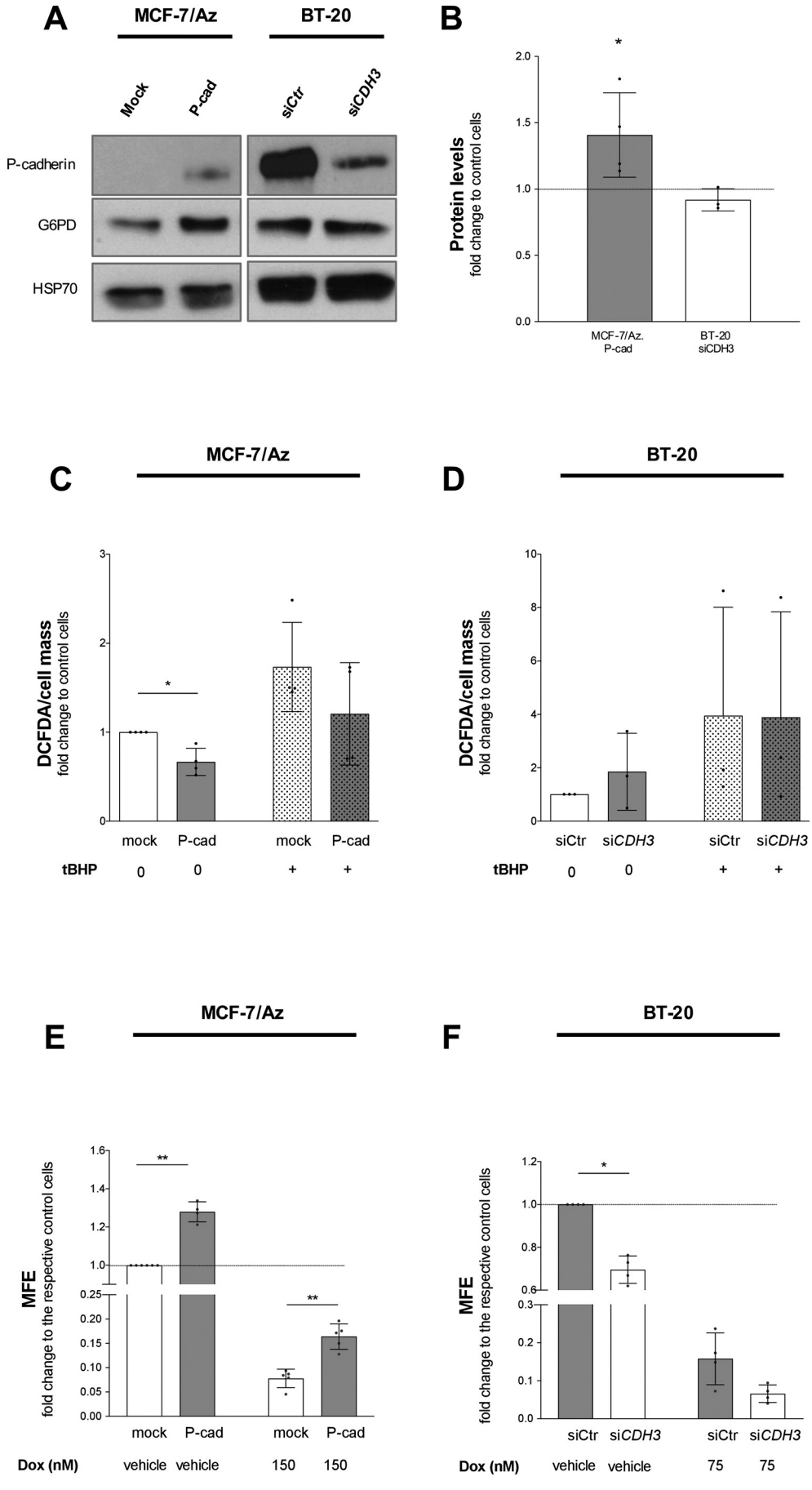

Fig. 2. P-cadherin expression promotes G6PD expression and modulates the oxidative stress of matrix-detached breast cancer cells. Western Blot representative image of G6PD (A) of both MCF-7/AZ and BT-20 model and the respective quantification (B), showing a significant increase of G6PD in matrix-detached MCF-7/AZ cells with overexpression of P-cadherin ($p = 0.0286$), in comparison with the control cells (A and B); No alterations were found in BT-20 cells (A and B); (Mean ± SD, N ≥ 3, unpaired Mann-Whitney test). The oxidative stress levels measured by DCFDA are statistically significant decreased in P-cadherin-overexpressing cells in comparison with MCF-7/AZ.mock cells ($p = 0.0286$) (C). Additionally, inhibition of P-cadherin expression in matrix-detached BT-20 cells leads to an increase of ROS production, when compared with the control cells (si*Ctr*), although the difference was not statistically significant (D). DCFDA data was normalized to the cell mass, measured by SRB assay; (Mean ± SD, $N = 3–4$, $n \geq 3$, Unpaired test Mann Whitney test). tBHP was used as positive control for DCF oxidation. Pre-treatment of breast cancer cells with DOX induced a substantial decrease in *anoikis*-resistance of all the cell lines evaluated (E and F). P-cadherin overexpression promoted *anoikis*-resistance in MCF-7/AZ cells when the cells were treated with 150 nM of DOX, since its expression led to a significant lower inhibition of MFE when comparing the effect of DOX on MCF-7/AZ.mock cells ($p = 0.0079$) (E). The same effect was observed in BT-20 model, in which 75 nM of DOX induced a decrease in MFE mainly in BT-20 cells with *CDH3* silencing, in comparison with the control cells (F), although not statistically significant; (Mean ± SD, N = 3–4, n ≥ 3, Unpaired test Mann Whitney test); ($*p < 0.0332$, $**p < 0.0021$ $***p < 0.0002$, $****p < 0.0001$).

expression plays a role in the resistance of matrix-detached breast cancer cells to pro-oxidative chemotherapeutic agents used in the clinical practice, such as doxorubicin (DOX) (Fig. 2E and F). As expected, MCF-7/AZ.P-cad cells treated only with the DMSO vehicle showed a 27% increased MFE ($p = 0.0022$), in comparison to the respective control cells; the same effect was observed in vehicle-treated BT-20 cells, where *CDH3* silencing showed a significant 30% decrease of MFE relative to control cells ($p = 0.0079$). The concentration of DOX used to treat both MCF-7/AZ and BT-20 cells was lower than the concentration that induced 50% of cell death in monolayer culture (Supplementary Fig. 5). Interestingly, the pre-treatment of breast cancer cells with DOX during 48 h induced a substantial decrease in *anoikis*-resistance of all the cell lines evaluated, in comparison to cells treated with DMSO (Fig. 2E and F). However, DOX was less effective in inhibiting survival in P-cadherin-overexpressing cells, in comparison to MCF-7/AZ.mock cells (84% vs 92% inhibition, respectively) ($p = 0.0079$), (Fig. 2E). Accordingly, DOX treatment of BT-20 cells led to a decrease in MFE, mainly in *CDH3*-silenced cells (84% vs 93% inhibition in siCtr vs siCDH3 cells, respectively), although the effect was not statistically significant (Fig. 2F).

These results suggest that P-cadherin overexpression protects cells from DOX treatment, probably by decreasing their oxidative stress levels in both MCF-7/AZ and BT-20 matrix-detached breast cancer cells.

3.3. P-cadherin expression regulates oxidative stress through the increase of antioxidant protection in matrix-detached breast cancer cells

In addition to the PPP antioxidant potential, cancer cells also respond to oxidative stress by the up-regulation of several detoxifying systems, such as glutathione, catalase and superoxide dismutase (SOD) systems. So, we evaluated whether P-cadherin would act as an *anoikis*-resistant factor in matrix-detached breast cancer cells through the induction of an antioxidant program. We started by measuring the glutathione antioxidant system (Fig. 3A and B). Surprisingly, we found that matrix-detached MCF-7/AZ.P-cad cells presented 36% lower GSH/GSSG levels in comparison with the respective control cells, although the difference was not statistically significant (Fig. 3A). No alterations were found in BT-20 cells in the same parameters (Fig. 3B). Concerning catalase activity, we observed a 26% increase in matrix-detached MCF-7/AZ.P-cad cells, suggesting an increased conversion of hydrogen peroxide into H_2O and O_2, in comparison to control cells (Fig. 3C). Accordingly, there was a 11% decrease of catalase activity in BT-20 after *CDH3* silencing (Fig. 3D). However, the differences in catalase activity in the two cell lines were not statistically significant. We also evaluated by western blot the expression of SOD1 and SOD2, which convert superoxide anion into H_2O_2 and O_2 (Fig. 3E, F and G). P-cadherin overexpression in detached MCF-7/AZ cells induced a 19% decrease in SOD1 ($p = 0.0010$), as well as a 36% increase of SOD2 ($p = 0.0021$) expression (Fig. 3E and F). We could also find that *CDH3* silencing in BT-20 cells induced a 16% decrease in SOD1 expression ($p < 0.0001$), while no differences were found for SOD2 expression (Fig. 3E and G).

These results demonstrate that P-cadherin expression maintains low levels of oxidative stress and consequent cellular damage, through increased catalase activity, as well as by regulating SOD1 and SOD2 expression.

3.4. P-cadherin overexpression is significantly associated with the expression of SOD1 and SOD2 antioxidant systems in human breast cancer samples

Similarly to P-cadherin, SOD2 expression is increased in basal-like breast carcinomas [25], being also responsible for the survival of circulating breast cancer cells, as well as for doxorubicin resistance, in basal-like breast cancer cell lines [25,26]. Thus, in order to validate the link between the expression of P-cadherin and the SOD antioxidants systems in breast cancer, we studied this association in a large series of formalin-fixed and paraffin-embedded invasive breast carcinomas (Fig. 4), previously described and characterized by our group [7,15]. Using immunohistochemistry, we observed a predominant cytoplasmic staining of SOD1 (Fig. 4A) in 50.9% (198/389) of the cases and a granular pattern of SOD2 expression (Fig. 4B) in 33.2% (138/416) of breast carcinomas. Interestingly, P-cadherin overexpression was found to be significantly associated with the very low or absent SOD1 expression ($p = 0.023$), as well as with the positive expression of SOD2 ($p = 0.039$) (Fig. 4C and D, respectively, and Supplementary Table 2). This association is also represented in Fig. 4E-G, where sequential slides of a breast carcinoma shows P-cadherin and SOD2 positivity, as well as SOD1 negativity. Moreover, no association was found between SOD1 and SOD2 expression with other members of classical cadherins family, such as E-cadherin (Supplementary Table 2), demonstrating specificity for P-cadherin.

The association between the expression of SOD1 and SOD2 with the classical breast cancer prognostic factors, as well as with molecular biomarkers and subtypes were also evaluated and are summarized in Supplementary Table 3. Although no significant associations were found between SOD1 and any prognostic or molecular factor, SOD2 expression was enriched in ER negative tumors ($p = 0.002$), as well as in CK5 and Vimentin expressing tumors ($p = 0.016$ and $p = 0.036$, respectively). Moreover, SOD1 and SOD2 expressing tumors showed a statistically significant increase in their proliferative index by their increased Ki67 staining ($p = 0.012$ and $p = 0.039$, respectively). Finally, we also observed an enrichment of SOD2 expression in tumors expressing the breast cancer stem cell marker CD49f, as well as in GLUT1 expressing tumors (Supplementary Table 4). With this data, we could demonstrate that breast carcinomas with aberrant expression of P-cadherin are significantly associated to tumors with a high percentage of cancer cells stained for SOD2 and deprived of SOD1 expression (Fig. 4).

Finally, since it was recently suggested that breast cancer cells harboring a ROS-resistant phenotype migrate from peri-necrotic regions to blood vessels oxygenated areas, being probably the cells with the ability to enter in circulation and form breast cancer distant metastasis [27], we further observed P-cadherin expression location in human primary invasive breast carcinomas. Interestingly, we found that P-cadherin was frequently expressed around oxygenated areas, near the blood vessels, and away from hypoxic areas, stained with HIF-1α (Fig. 4H). We also observed the same expression pattern between P-cadherin and HIF-1α downstream target GLUT1, as we can see in Fig. 4I, where both proteins are expressed in different areas of primary breast carcinomas.

4. Discussion

Cell-cell adhesion is mainly mediated through cadherins, which expression and function are largely implicated in cancer cell invasion and progression. Actually, we demonstrated that P-cadherin expression is an independent indicator of poor prognosis in breast cancer patients and a putative useful biomarker for axillary-based breast cancer decisions in the clinical practice [4,8,13]. The tumorigenic and invasive role of this adhesion molecule has been partially attributed to its ability to enhance cancer stem-like characteristics, such as in vitro mammosphere-forming efficiency, as well as resistance to *anoikis* and to x-ray radiation [7,13]. In accordance, in the normal context, P-cadherin expression has been proposed to be a marker of stem or progenitor cells in epithelial tissues [28].

Interestingly, cell-cell adhesion is gaining a new recognition in the metabolic necessities of cancer cells along the metastatic cascade [16,29]. In accordance, we described a link between P-cadherin and breast cancer cell metabolism, by its association with hypoxic, glycolytic and acid-resistant human breast carcinomas [15]. We reported that breast cancer cell populations enriched for P-cadherin showed concomitant expression of HIF-1α, CAIX, and GLUT1, demonstrating

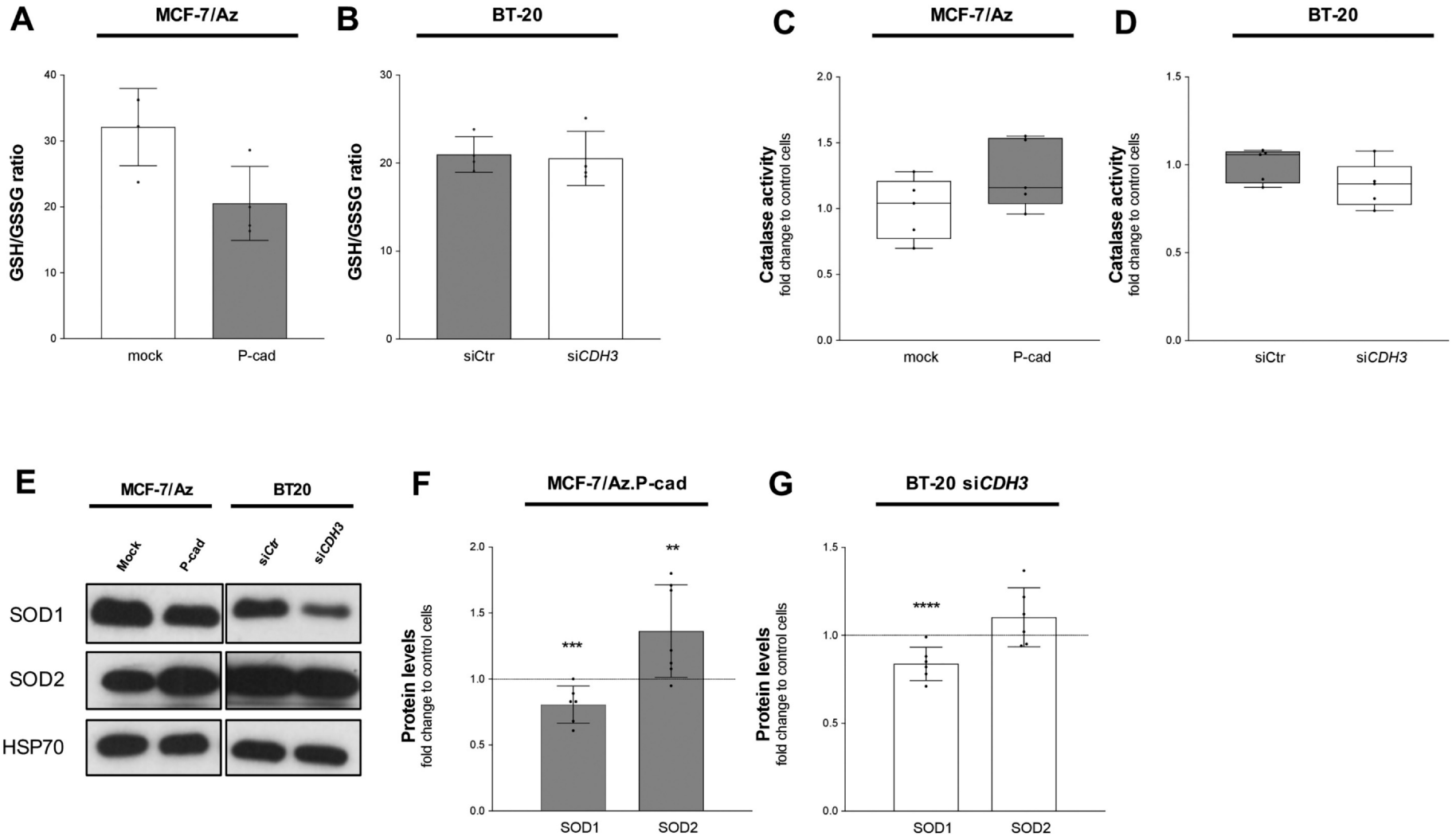

Fig. 3. P-cadherin expression promotes antioxidant program in matrix-detached breast cancer cells. Glutathione redox balance, measured through GSH/GSSG ratio, is decreased in P-cadherin-overexpressing matrix-detached cells, in comparison with MCF7/AZ.mock control cells (A), while no difference was found in BT-20 model (B); (Mean ± SD, N = 3–4, n ≥ 3, Unpaired test Mann Whitney test). Catalase activity is increased in MCF-7/AZ.P-cad vs MCF-7/AZ.mock cells (C) and slightly decreased in *CDH3*-silenced BT-20 vs BT-20 siCtr cells (D); (Mean ± SD, N = 3–4, n ≥ 3, Unpaired test Mann Whitney test). Western Blot representative image of SOD1 and SOD2 (E) of both MCF-7/AZ and BT-20 model and the respective quantification (F and G), showing a significant decrease of SOD1 and an increase of SOD2 ($p = 0.0010$ and $p = 0.0021$, *respectively)*, in matrix-detached MCF-7/AZ cells with overexpression of P-cadherin, in comparison with the control cells (F); Additionally, SOD1 was significantly decreased in matrix-detached BT-20 si*CDH3* vs BT-20 siCtr cells ($p < 0.0001$) (G); (Mean ± SD, $N \geq 3$, unpaired Mann-Whitney test); (*p < 0.0332, **p < 0.0021 ***p < 0.0002, ****p < 0.0001).

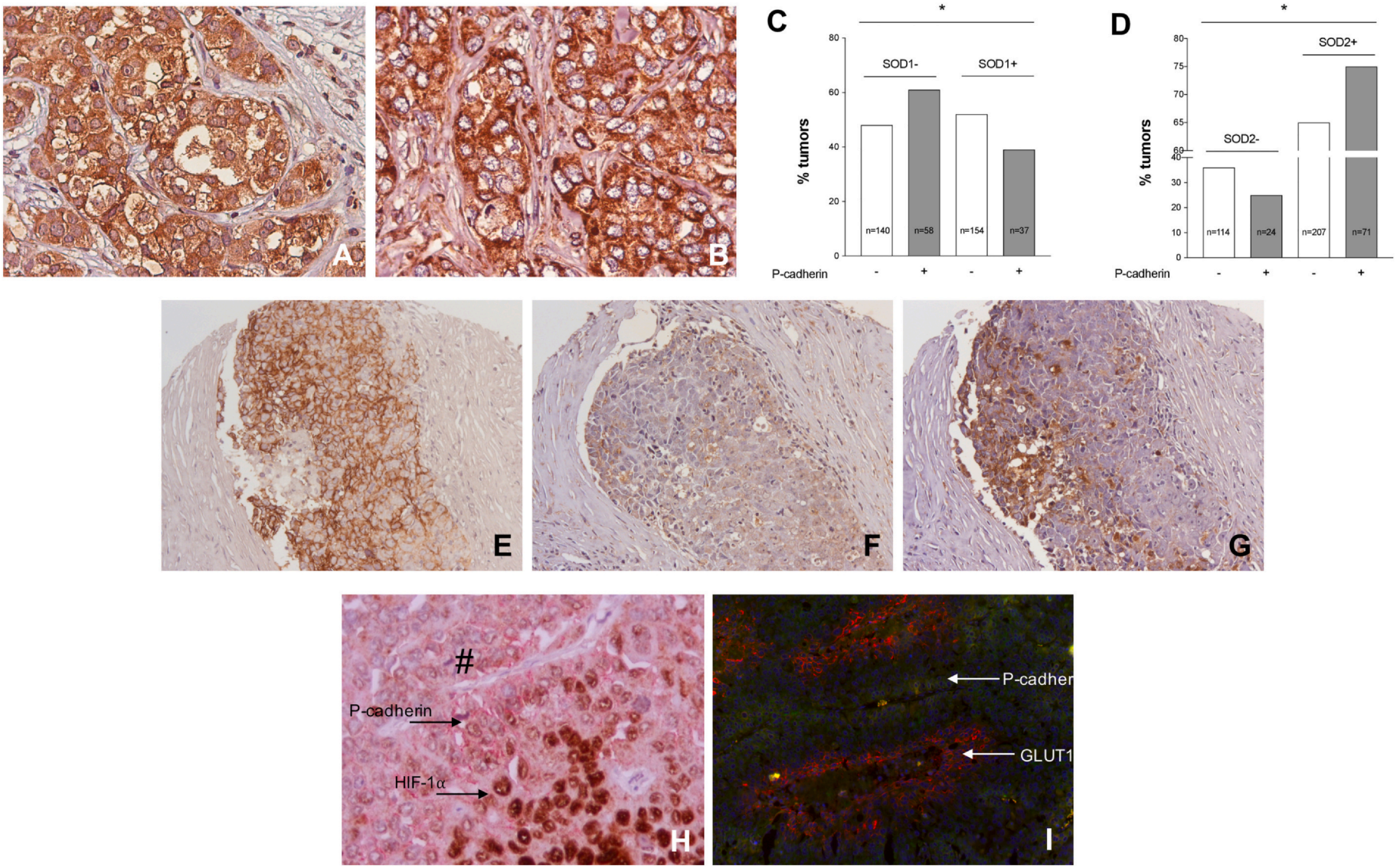

Fig. 4. Aberrant P-cadherin expression is associated with antioxidant proteins SOD1 and SOD2 in human primary invasive breast carcinomas. Immunoexpression of SOD1 (A) and SOD2 (B) in a human primary invasive breast carcinoma (400× magnification). P-cadherin overexpression was significantly associated with the lack of expression SOD1 *($p = 0.0023$)* (C), as well as with the expression of SOD2 *($p = 0.0039$)* (D), in a series of primary invasive breast carcinomas; $\chi 2$ test, $^*p < 0.05$. A representative sample shows P-cadherin-positivity/ SOD1-negativity/ SOD2-positivity (E, F and G, respectively) in sequential slides of the same breast carcinoma (200× magnification). Moreover, by immunohistochemistry double-staining (H and I), we observed that membrane P-cadherin expression (Red) was frequently found in oxygenated areas near blood vessels (#) and not in hypoxic areas identified by nuclear HIF-1α (H). Moreover, using immunofluorescence, we also observed consistent different localizations of P-cadherin (green) and HIF-1α downstream target GLUT1 (Red) (I);

the putative glycolytic behavior of these cancer cells [15]. In the present work, we investigated whether the reported role of P-cadherin in the survival of cancer cells, especially while in circulation, can be due to its ability to modulate the metabolism and oxidative stress of matrix-detached breast cancer cells.

Using experimental conditions mimicking anchorage-independent conditions of circulating cancer cells, we propose that P-cadherin expression rewires the metabolic flux towards the oxidative arm of PPP, by increasing G6PD expression, as well as through the increased PDK4-induced PDH phosphorylation, inhibiting pyruvate oxidation to acetyl-coA in matrix-detached breast cancer cells. Cancer cells with increased glycolytic, as well as increased PPP flux, have higher sensitivity to DCA [30,31]. Accordingly, we also found that P-cadherin-enriched matrix-detached breast cancer cells are more sensitive to DCA-induced *anoikis*, since these cells present increased DCA-target PDK4 and increased expression of PPP rate-limiting protein, G6PD. Importantly, we also found that P-cadherin expression decreases oxidative stress in these cells through the modulation of SOD and catalase antioxidant protection systems, being probably responsible for the resistance to pro-oxidant doxorubicin-induced *anoikis*.

These results are in accordance with previously published data, which demonstrated that breast cancer cells enriched for stem cell characteristics exhibit pro-glycolytic metabolic skills, low levels of oxidative stress and increased antioxidant protection, being able to escape *anoikis*, survive in circulation, being refractory to pro-oxidant therapies and promoting metastasis [29,30,32,33]. Moreover, these glycolytic breast cancer stem cells (BCSCs) are highly responsive to DCA, which unlocks cells from death resistance by the inhibition of the PDK-pPDH checkpoint, redirecting ATP production from glycolysis to mitochondrial oxidative phosphorylation and promoting oxidative stress-induced cell death [34]. Accordingly, pluripotent human embryonic stem cells (hESC) are also highly responsive to DCA, as well as different CSCs [35–38], whose treatment leads to a decrease in the expression of the CSC markers CD24/CD44/EpCAM and of the spheroid forming efficiency, as well as to an increase of chemo- and radiotherapy sensitivity [38–40]. In breast cancer, DCA decreases BCSC clonogenicity in 3D spheroid culture systems, being this effect associated with decreased PDH expression and activity [30]. Increased PDK-pPDH circuit favors a glycolytic metabolism and promotes pluripotency in BCSCs. Thus, in accordance with our previous suggestion of a glycolytic phenotype in P-cadherin-overexpressing BCSC populations [15], this work shows that DCA targets preferentially P-cadherin-enriched matrix-detached breast cancer cells, with increased PDK4-induced PDH phosphorylation. This effect is probably due to DCA-induced reprograming from a predominantly glycolytic metabolism, which is required for ECM detached survival, to mitochondrial oxidative phosphorylation, increasing oxidative stress and decreasing *anoikis*-resistance.

Similarly to P-cadherin, high levels of PDK4 expression are also associated with poor prognosis and therapy resistance in breast cancer [41,42]. Interestingly, PDK4 seems to be the most important PDK isoform for the maintenance of stem-like features and *anoikis*-resistance upon ECM detachment, either in human mammary cells, as well as in breast cancer and other cancer stem cell models [39,40,43–45]. Moreover, our results also suggest that P-cadherin-enriched matrix-detached breast cancer cells may have increased metabolic flux into the PPP, as observed by the G6PD expression in these cells, as well as by a slight decrease in basal glycolysis flux. This redirection of the metabolic flux away from lactate-producing glycolysis, makes OCR and ECAR differences almost imperceptible using extracellular measurements [33,46]. Nevertheless, energy maps using the Seahorse data in unstressed and stressed cells showed that P-cadherin overexpression in MCF-7/AZ breast cancer cells led to a stronger up-regulation of glycolytic metabolism as compared to control cells. This suggests a more robust glycolytic machinery triggered by P-cadherin overexpression, although a detailed comprehensive analysis of the distinct metabolites involved would be a valuable approach to understand its effect in matrix-detached breast cancer cells. It would be important to specifically understand if mitochondrial oxidative phosphorylation is being fueled by different metabolites, such as glutamine or lactate, or by other metabolic substrates derived from alternative biosynthetic pathways, which is a limitation of this study.

Remarkably, upon ECM detachment in systemic metastatic dissemination, cancer cells largely increase their ROS levels. Thus, in order to escape oxidative stress-induced *anoikis*, cancer cells adapt their metabolism and increase their antioxidant defense network, promoting pluripotency, survival in circulation and promoting the establishment of metastasis [45]. Specifically, the increased antioxidant ability exhibited by BCSCs is one of the major contributing factors for resistance to pro-oxidant radiotherapy and chemotherapy used in clinical practice, such as DOX [32,33]. In accordance with the recognized role of P-cadherin in *anoikis*-resistance, as well as in the resistance to x-ray-induced breast cancer cell death [7], we observed that P-cadherin regulates intracellular oxidative stress of matrix-detached breast cancer cells. Furthermore, we also observed that P-cadherin protects matrix-detached breast cancer cells from *anoikis* after DOX treatment, probably due to the impairment of oxidative stress.

The most important antioxidant enzymes in breast cancer cells are SOD, catalase and glutathione peroxidase (GPx), where SOD converts superoxide radical into hydrogen peroxide and oxygen, whereas the catalase and peroxidases convert hydrogen peroxide into water. Surprisingly, we found that matrix-detached MCF7/AZ.P-cad cells presented lower levels of GSH/GSSG levels in comparison to control cells, which may contradict increased NADPH supply from the PPP, thus leading to higher GSH regeneration and antioxidant effects in P-cadherin-enriched matrix-detached cells. However, this complex system and the maintenance of the GSH/GSSG requires the activity of several other enzymes and cofactors to function at its high efficiency. Another explanation is that increased NADPH originated from the PPP is instead used for reductive biosynthesis in P-cadherin-overexpressing cells or as a substrate for NADPH quinone oxidoreductase 1, which is involved in cancer antioxidant defense and previously considered to have an important role in anchorage-independent survival of cancer cells [47]. To support the idea of increased antioxidant activity in P-cadherin-overexpressing cells, we also investigated SOD and catalase, two other important antioxidant systems responsible for *anoikis*-resistance in breast cancer cells after ECM-detachment [48]. We observed increased catalase activity in matrix-detached MCF-7/AZ-P-cad cells, while *CDH3* silencing led to a decrease of catalase activity in BT-20. These results indicate that P-cadherin promotes increased hydrogen peroxide detoxification in matrix-detached breast cancer cells. Moreover, P-cadherin expression induced a decrease in SOD1 and an increase of SOD2 expression in matrix-detached MCF-7/AZ cells. In BT-20 cells, *CDH3* silencing induced a decrease in SOD1, but no alterations in SOD2 expression, suggesting that P-cadherin regulates oxidative stress in this cell line specifically through SOD1.

Importantly, we were able to validate the association between P-cadherin and SODs expression in human samples. Using a large series of human primary invasive breast carcinomas, we found that P-cadherin overexpression was significantly associated with negative or low expression of SOD1, as well as with the presence SOD2 expression. We believe that, in accordance with the described SOD1 to SOD2 switch [49], SOD1 downregulation might be maintaining ROS in the required levels to conduct ROS mediated signaling. Moreover, similarly to P-cadherin expression in human breast carcinomas, SOD2 was already associated with high histological grade and poorly differentiated tumors, hormone receptors negativity, p53 expression, decreased disease free survival, as well as with poor prognosis molecular subtypes, such as basal-like and claudin low breast cancer subtypes [25,50–53]. Still, micro and macro-metastasis presents higher levels of SOD2 when compared to their matched primary breast tumor [53]. Accordingly, we also found enriched SOD2 expression in ER negative and proliferative tumors, as well as in tumors harboring a basal-like phenotype.

Interestingly, SOD2 expression was also associated with P-cadherin, CD49f and GLUT1 expressing tumors, supporting the antioxidant activity of P-cadherin-overexpressing breast carcinomas with a glycolytic, undifferentiated and stem-like phenotype.

Although P-cadherin signaling is still far from being totally understood, we and others have described some of the mechanisms that could underlie the effects described in this report [6,8,11,15]. We have previously shown that P-cadherin overexpression leads to the activation of FAK, Src and AKT Kinases [8], and that P-cadherin-induced tumorigenic and metastatic ability are suppressed by Src activity suppression with dasatinib [11]. Importantly, Src activation, also described to promote *anoikis*-resistance, attenuates PDH activity and ROS production, and consequently, Src inhibitors sensitize breast cancer cells to Doxorubicin [54]. Additionally, SOD2 expression have been linked with increased expression and activity of MMPs, as well as with increased angiogenesis and migration via PI3Kinase and FAK signaling cascades. Dismutase activity of SOD2 has been also directly linked to tumor cell radio- and chemo-resistance [55]. However, the implication of Src, FAK and AKT Kinases in the mechanism underlying the glycolytic and antioxidant mechanism induced by P-cadherin expression in breast cancer cells remains speculative and needs further validation in future studies.

We further investigated the location of P-cadherin expression in breast carcinomas and found that it was frequently expressed around oxygenated areas, near the blood vessels, and away from hypoxic areas. Interestingly, Godet et al. has recently shown that peri-necrotic cancer cells exposed to intratumoral hypoxia exhibit a ROS-resistant phenotype, have increased ability to survive in the bloodstream and enhanced breast cancer lung metastasis ability [27]. Since we have previously demonstrated that nuclear HIF-1α induces P-cadherin expression [15], and it is also known that HIF-1α expressing cells in hypoxic regions can modulate the behavior of cancer cells in non-hypoxic regions, such as their anchorage-independent abilities [56], we believe that P-cadherin expression is functioning as a survival signal to circulating tumor cells.

In conclusion, the present study supports P-cadherin's putative role in the survival of circulating tumor cells. However, additional evidence would be required in supplementary breast cancer models, in order to establish the molecular mechanism behind this function, as well as the specific role of PDK4, SOD1 and SOD2 in P-cadherin-induced PPP and antioxidant phenotype in matrix-detached breast cancer cells. We are aware of the lack of direct evidence implicating P-cadherin expression in the *anoikis*-resistance specifically due to protection against DOX-induced oxidative stress. Anyway, we describe for the first time the glycolytic and antioxidant role of P-cadherin in matrix-detached breast cancer cells, which might impact their ability to resist to pro-oxidant therapy, to enter and survive in circulation, and ultimately to lead to distant metastasis. Thus, the targeting of this adhesion molecule can constitute a promising strategy specifically to impair the progression of breast cancer in advanced stages of this disease.

Supplementary data to this article can be found online at https://doi.org/10.1016/j.bbadis.2020.165964.

CRediT authorship contribution statement

Bárbara Sousa: Conceptualization, Methodology, Formal analysis, Investigation, Visualization, Writing- Original draft; **Joana Pereira:** Investigation; **Ricardo Marques:** Formal analysis, Investigation, Writing- Review and Editing; **Luís F. Grilo:** Methodology; **Susana P. Pereira:** Methodology; **Vilma A. Sardão:** Methodology; **Fernando Schmitt:** Investigation, Resources; **Paulo Oliveira:** Conceptualization, Writing- Review and Editing, Supervision; **Joana Paredes:** Conceptualization, Writing- Original draft, Writing- Review and Editing, Supervision, Visualization, Funding acquisition, Project administration.

Declaration of competing interest

The authors declare that they have no known competing financial interests or personal relationships that could have appeared to influence the work reported in this paper.

Acknowledgments

This work is funded by FEDER—Fundo Europeu de Desenvolvimento Regional through the COMPETE 2020—Operational Programme for Competitiveness and Internationalisation (POCI), Portugal 2020, and by FCT- Fundação para a Ciência e a Tecnologia, under the project POCI-01-0145-FEDER-016390 and UIDB/04539/2020. Ipatimup integrates the i3S Research Unit, which is partially supported by FCT in the framework of the project "Institute for Research and Innovation in Health Sciences" (POCI-01-0145-FEDER-007274). FCT funded the research grants of JP (SFRH/BD/143533/2019) and SPP (SFRH/BPD/116061/2016). We thank to Dr. Jorge F Cameselle-Teijeiro, at Complejo Hospitalario Universitário de Vigo (CHUVI), Vigo, Spain, for the FFPE breast cancer samples. We also thank to Dr. Inês Baldeiras and João Martins for their advice regarding glutathione and catalase activity determination, respectively. Finally, we thank to Patricia Oliveira for the help in graphical arrangements of this work.

References

[1] J. Paredes, J. Figueiredo, A. Albergaria, P. Oliveira, J. Carvalho, A.S. Ribeiro, J. Caldeira, A.M. Costa, J. Simoes-Correia, M.J. Oliveira, H. Pinheiro, S.S. Pinho, R. Mateus, C.A. Reis, M. Leite, M.S. Fernandes, F. Schmitt, F. Carneiro, C. Figueiredo, C. Oliveira, R. Seruca, Epithelial E- and P-cadherins: role and clinical significance in cancer, Biochim. Biophys. Acta 1826 (2012) 297–311.

[2] W. Yu, L. Yang, T. Li, Y. Zhang, Cadherin signaling in cancer: its functions and role as a therapeutic target, Front. Oncol. 9 (2019) 989.

[3] J. Paredes, A. Albergaria, J.T. Oliveira, C. Jeronimo, F. Milanezi, F.C. Schmitt, P-cadherin overexpression is an indicator of clinical outcome in invasive breast carcinomas and is associated with CDH3 promoter hypomethylation, Clin. Cancer Res. 11 (2005) 5869–5877.

[4] A.F. Vieira, M.R. Dionisio, M. Gomes, J.F. Cameselle-Teijeiro, M. Lacerda, I. Amendoeira, F. Schmitt, J. Paredes, P-cadherin: a useful biomarker for axillary-based breast cancer decisions in the clinical practice, Mod. Pathol. 30 (2017) 698–709.

[5] J. Paredes, C. Stove, V. Stove, F. Milanezi, V. Van Marck, L. Derycke, M. Mareel, M. Bracke, F. Schmitt, P-cadherin is up-regulated by the antiestrogen ICI 182,780 and promotes invasion of human breast cancer cells, Cancer Res. 64 (2004) 8309–8317.

[6] A.S. Ribeiro, A. Albergaria, B. Sousa, A.L. Correia, M. Bracke, R. Seruca, F.C. Schmitt, J. Paredes, Extracellular cleavage and shedding of P-cadherin: a mechanism underlying the invasive behaviour of breast cancer cells, Oncogene 29 (2010) 392–402.

[7] A.F. Vieira, S. Ricardo, M.P. Ablett, M.R. Dionisio, N. Mendes, A. Albergaria, G. Farnie, R. Gerhard, J.F. Cameselle-Teijeiro, R. Seruca, F. Schmitt, R.B. Clarke, J. Paredes, P-cadherin is coexpressed with CD44 and CD49f and mediates stem cell properties in basal-like breast cancer, Stem Cells 30 (2012) 854–864.

[8] A.F. Vieira, A.S. Ribeiro, M.R. Dionisio, B. Sousa, A.R. Nobre, A. Albergaria, A. Santiago-Gomez, N. Mendes, R. Gerhard, F. Schmitt, R.B. Clarke, J. Paredes, P-cadherin signals through the laminin receptor alpha6beta4 integrin to induce stem cell and invasive properties in basal-like breast cancer cells, Oncotarget 5 (2014) 679–692.

[9] A.S. Ribeiro, B. Sousa, L. Carreto, N. Mendes, A.R. Nobre, S. Ricardo, A. Albergaria, J.F. Cameselle-Teijeiro, R. Gerhard, O. Soderberg, R. Seruca, M.A. Santos, F. Schmitt, J. Paredes, P-cadherin functional role is dependent on E-cadherin cellular context: a proof of concept using the breast cancer model, J. Pathol. 229 (2013) 705–718.

[10] A.S. Ribeiro, F.A. Carvalho, J. Figueiredo, R. Carvalho, T. Mestre, J. Monteiro, A.F. Guedes, M. Fonseca, J. Sanches, R. Seruca, N.C. Santos, J. Paredes, Atomic force microscopy and graph analysis to study the P-cadherin/SFK mechanotransduction signalling in breast cancer cells, Nanoscale 8 (2016) 19390–19401.

[11] A.S. Ribeiro, A.R. Nobre, N. Mendes, J. Almeida, A.F. Vieira, B. Sousa, F.A. Carvalho, J. Monteiro, A. Polonia, M. Fonseca, J.M. Sanches, N.C. Santos, R. Seruca, J. Paredes, SRC inhibition prevents P-cadherin mediated signaling and function in basal-like breast cancer cells, Cell Commun Signal 16 (2018) 75.

[12] A.S. Ribeiro, J. Paredes, P-cadherin linking breast cancer stem cells and invasion: a promising marker to identify an "intermediate/metastable" EMT state, Front. Oncol. 4 (2014) 371.

[13] A.F. Vieira, J. Paredes, P-cadherin and the journey to cancer metastasis, Mol. Cancer 14 (2015) 178.

[14] K. Campbell, Contribution of epithelial-mesenchymal transitions to organogenesis and cancer metastasis, Curr. Opin. Cell Biol. 55 (2018) 30–35.
[15] B. Sousa, A.S. Ribeiro, A.R. Nobre, N. Lopes, D. Martins, C. Pinheiro, A.F. Vieira, A. Albergaria, R. Gerhard, F. Schmitt, F. Baltazar, J. Paredes, The basal epithelial marker P-cadherin associates with breast cancer cell populations harboring a glycolytic and acid-resistant phenotype, BMC Cancer 14 (2014) 734.
[16] B. Sousa, J. Pereira, J. Paredes, The Crosstalk between Cell Adhesion and Cancer Metabolism, Int J Mol Sci, 20, (2019).
[17] V. Vichai, K. Kirtikara, Sulforhodamine B colorimetric assay for cytotoxicity screening, Nat. Protoc. 1 (2006) 1112–1116.
[18] I. Rahman, A. Kode, S.K. Biswas, Assay for quantitative determination of glutathione and glutathione disulfide levels using enzymatic recycling method, Nat. Protoc. 1 (2006) 3159–3165.
[19] H. Aebi, Catalase in vitro, Methods Enzymol. 105 (1984) 121–126.
[20] B. Sousa, J. Paredes, F. Milanezi, N. Lopes, D. Martins, R. Dufloth, D. Vieira, A. Albergaria, L. Veronese, V. Carneiro, S. Carvalho, J.L. Costa, L. Zeferino, F. Schmitt, P-cadherin, vimentin and CK14 for identification of basal-like phenotype in breast carcinomas: an immunohistochemical study, Histol. Histopathol. 25 (2010) 963–974.
[21] S. Ricardo, A.F. Vieira, R. Gerhard, D. Leitao, R. Pinto, J.F. Cameselle-Teijeiro, F. Milanezi, F. Schmitt, J. Paredes, Breast cancer stem cell markers CD44, CD24 and ALDH1: expression distribution within intrinsic molecular subtype, J. Clin. Pathol. 64 (2011) 937–946.
[22] A. Albergaria, C. Resende, A.R. Nobre, A.S. Ribeiro, B. Sousa, J.C. Machado, R. Seruca, J. Paredes, F. Schmitt, CCAAT/enhancer binding protein beta (C/EBPbeta) isoforms as transcriptional regulators of the pro-invasive CDH3/P-cadherin gene in human breast cancer cells, PLoS One 8 (2013) e55749.
[23] E.D. Michelakis, L. Webster, J.R. Mackey, Dichloroacetate (DCA) as a potential metabolic-targeting therapy for cancer, Br. J. Cancer 99 (2008) 989–994.
[24] A. Stincone, A. Prigione, T. Cramer, M.M. Wamelink, K. Campbell, E. Cheung, V. Olin-Sandoval, N.M. Gruning, A. Kruger, M. Tauqeer Alam, M.A. Keller, M. Breitenbach, K.M. Brindle, J.D. Rabinowitz, M. Ralser, The return of metabolism: biochemistry and physiology of the pentose phosphate pathway, Biol. Rev. Camb. Philos. Soc. 90 (2015) 927–963.
[25] A.P. Kumar, S.Y. Loo, S.W. Shin, T.Z. Tan, C.B. Eng, R. Singh, T.C. Putti, C.W. Ong, M. Salto-Tellez, B.C. Goh, J.I. Park, J.P. Thiery, S. Pervaiz, M.V. Clement, Manganese superoxide dismutase is a promising target for enhancing chemosensitivity of basal-like breast carcinoma, Antioxid. Redox Signal. 20 (2014) 2326–2346.
[26] A. Fu, S. Ma, N. Wei, B.X. Tan, E.Y. Tan, K.Q. Luo, High expression of MnSOD promotes survival of circulating breast cancer cells and increases their resistance to doxorubicin, Oncotarget 7 (2016) 50239–50257.
[27] I. Godet, Y.J. Shin, J.A. Ju, I.C. Ye, G. Wang, D.M. Gilkes, Fate-mapping post-hypoxic tumor cells reveals a ROS-resistant phenotype that promotes metastasis, Nat. Commun. 10 (2019) 4862.
[28] G.L. Radice, M.C. Ferreira-Cornwell, S.D. Robinson, H. Rayburn, L.A. Chodosh, M. Takeichi, R.O. Hynes, Precocious mammary gland development in P-cadherin-deficient mice, J. Cell Biol. 139 (1997) 1025–1032.
[29] I. Elia, G. Doglioni, S.M. Fendt, Metabolic hallmarks of metastasis formation, Trends Cell Biol. 28 (2018) 673–684.
[30] W. Feng, A. Gentles, R.V. Nair, M. Huang, Y. Lin, C.Y. Lee, S. Cai, F.A. Scheeren, A.H. Kuo, M. Diehn, Targeting unique metabolic properties of breast tumor initiating cells, Stem Cells 32 (2014) 1734–1745.
[31] G. De Preter, M.A. Neveu, P. Danhier, L. Brisson, V.L. Payen, P.E. Porporato, B.F. Jordan, P. Sonveaux, B. Gallez, Inhibition of the pentose phosphate pathway by dichloroacetate unravels a missing link between aerobic glycolysis and cancer cell proliferation, Oncotarget 7 (2016) 2910–2920.
[32] T.M. Phillips, W.H. McBride, F. Pajonk, The response of CD24(−/low)/CD44+ breast cancer-initiating cells to radiation, J. Natl. Cancer Inst. 98 (2006) 1777–1785.
[33] M. Diehn, R.W. Cho, N.A. Lobo, T. Kalisky, M.J. Dorie, A.N. Kulp, D. Qian, J.S. Lam, L.E. Ailles, M. Wong, B. Joshua, M.J. Kaplan, I. Wapnir, F.M. Dirbas, G. Somlo, C. Garberoglio, B. Paz, J. Shen, S.K. Lau, S.R. Quake, J.M. Brown, I.L. Weissman, M.F. Clarke, Association of reactive oxygen species levels and radioresistance in cancer stem cells, Nature 458 (2009) 780–783.
[34] S. Bonnet, S.L. Archer, J. Allalunis-Turner, A. Haromy, C. Beaulieu, R. Thompson, C.T. Lee, G.D. Lopaschuk, L. Puttagunta, S. Bonnet, G. Harry, K. Hashimoto, C.J. Porter, M.A. Andrade, B. Thebaud, E.D. Michelakis, A mitochondria-K+ channel axis is suppressed in cancer and its normalization promotes apoptosis and inhibits cancer growth, Cancer Cell 11 (2007) 37–51.
[35] A.S. Rodrigues, M. Correia, A. Gomes, S.L. Pereira, T. Perestrelo, M.I. Sousa, J. Ramalho-Santos, Dichloroacetate, the pyruvate dehydrogenase complex and the modulation of mESC pluripotency, PLoS One 10 (2015) e0131663.
[36] R. Loureiro, S. Magalhaes-Novais, K.A. Mesquita, I. Baldeiras, I.S. Sousa, L.C. Tavares, I.A. Barbosa, P.J. Oliveira, I. Vega-Naredo, Melatonin antiproliferative effects require active mitochondrial function in embryonal carcinoma cells, Oncotarget 6 (2015) 17081–17096.
[37] I. Vega-Naredo, R. Loureiro, K.A. Mesquita, I.A. Barbosa, L.C. Tavares, A.F. Branco, J.R. Erickson, J. Holy, E.L. Perkins, R.A. Carvalho, P.J. Oliveira, Mitochondrial metabolism directs stemness and differentiation in P19 embryonal carcinoma stem cells, Cell Death Differ 21 (2014) 1560–1574.
[38] T. Tataranni, F. Agriesti, C. Pacelli, V. Ruggieri, I. Laurenzana, C. Mazzoccoli, G.D. Sala, C. Panebianco, V. Pazienza, N. Capitanio, C. Piccoli, Dichloroacetate Affects Mitochondrial Function and Stemness-Associated Properties in Pancreatic Cancer Cell Lines, Cells, 8, (2019).
[39] K. Fekir, H. Dubois-Pot-Schneider, R. Desert, Y. Daniel, D. Glaise, C. Rauch, F. Morel, B. Fromenty, O. Musso, F. Cabillic, A. Corlu, Retrodifferentiation of human tumor hepatocytes to stem cells leads to metabolic reprogramming and chemoresistance, Cancer Res. 79 (2019) 1869–1883.
[40] T. Tataranni, C. Piccoli, Dichloroacetate (DCA) and cancer: an overview towards clinical applications, Oxidative Med. Cell. Longev. 2019 (2019) 8201079.
[41] M.R. Guda, S. Asuthkar, C.M. Labak, A.J. Tsung, I. Alexandrov, M.J. Mackenzie, D.V. Prasad, K.K. Velpula, Targeting PDK4 inhibits breast cancer metabolism, Am. J. Cancer Res. 8 (2018) 1725–1738.
[42] W. Walter, J. Thomalla, J. Bruhn, D.H. Fagan, C. Zehowski, D. Yee, A. Skildum, Altered regulation of PDK4 expression promotes antiestrogen resistance in human breast cancer cells, Springerplus 4 (2015) 689.
[43] S. Kamarajugadda, L. Stemboroski, Q. Cai, N.E. Simpson, S. Nayak, M. Tan, J. Lu, Glucose oxidation modulates anoikis and tumor metastasis, Mol. Cell. Biol. 32 (2012) 1893–1907.
[44] A.R. Grassian, C.M. Metallo, J.L. Coloff, G. Stephanopoulos, J.S. Brugge, Erk regulation of pyruvate dehydrogenase flux through PDK4 modulates cell proliferation, Genes Dev. 25 (2011) 1716–1733.
[45] Z.T. Schafer, A.R. Grassian, L. Song, Z. Jiang, Z. Gerhart-Hines, H.Y. Irie, S. Gao, P. Puigserver, J.S. Brugge, Antioxidant and oncogene rescue of metabolic defects caused by loss of matrix attachment, Nature 461 (2009) 109–113.
[46] S.A. Mookerjee, D.G. Nicholls, M.D. Brand, Determining maximum glycolytic capacity using extracellular flux measurements, PLoS One 11 (2016) e0152016.
[47] M. Shimokawa, T. Yoshizumi, S. Itoh, N. Iseda, K. Sakata, K. Yugawa, T. Toshima, N. Harada, T. Ikegami, M. Mori, Modulation of Nqo1 activity intercepts anoikis resistance and reduces metastatic potential of hepatocellular carcinoma, Cancer Sci. 111 (2020) 1228–1240.
[48] C.A. Davison, S.M. Durbin, M.R. Thau, V.R. Zellmer, S.E. Chapman, J. Diener, C. Wathen, W.M. Leevy, Z.T. Schafer, Antioxidant enzymes mediate survival of breast cancer cells deprived of extracellular matrix, Cancer Res. 73 (2013) 3704–3715.
[49] L. Papa, M. Hahn, E.L. Marsh, B.S. Evans, D. Germain, SOD2 to SOD1 switch in breast cancer, J. Biol. Chem. 289 (2014) 5412–5416.
[50] Y. Soini, M. Vakkala, K. Kahlos, P. Paakko, V. Kinnula, MnSOD expression is less frequent in tumour cells of invasive breast carcinomas than in in situ carcinomas or non-neoplastic breast epithelial cells, J. Pathol. 195 (2001) 156–162.
[51] T. Sorlie, C.M. Perou, R. Tibshirani, T. Aas, S. Geisler, H. Johnsen, T. Hastie, M.B. Eisen, M. van de Rijn, S.S. Jeffrey, T. Thorsen, H. Quist, J.C. Matese, P.O. Brown, D. Botstein, P. Eystein Lonning, A.L. Borresen-Dale, Gene expression patterns of breast carcinomas distinguish tumor subclasses with clinical implications, Proc. Natl. Acad. Sci. U. S. A. 98 (2001) 10869–10874.
[52] E. Tsanou, E. Ioachim, E. Briasoulis, K. Damala, A. Charchanti, V. Karavasilis, N. Pavlidis, N.J. Agnantis, Immunohistochemical expression of superoxide dismutase (MnSOD) anti-oxidant enzyme in invasive breast carcinoma, Histol. Histopathol. 19 (2004) 807–813.
[53] S. Kamarajugadda, Q. Cai, H. Chen, S. Nayak, J. Zhu, M. He, Y. Jin, Y. Zhang, L. Ai, S.S. Martin, M. Tan, J. Lu, Manganese superoxide dismutase promotes anoikis resistance and tumor metastasis, Cell Death Dis. 4 (2013) e504.
[54] Y. Jin, Q. Cai, A.K. Shenoy, S. Lim, Y. Zhang, S. Charles, M. Tarrash, X. Fu, S. Kamarajugadda, J.G. Trevino, M. Tan, J. Lu, Src drives the Warburg effect and therapy resistance by inactivating pyruvate dehydrogenase through tyrosine-289 phosphorylation, Oncotarget 7 (2016) 25113–25124.
[55] N. Hempel, P.M. Carrico, J.A. Melendez, Manganese superoxide dismutase (Sod2) and redox-control of signaling events that drive metastasis, Anti Cancer Agents Med. Chem. 11 (2011) 191–201.
[56] H. Harrison, H.J. Pegg, J. Thompson, C. Bates, P. Shore, HIF1-alpha expressing cells induce a hypoxic-like response in neighbouring cancer cells, BMC Cancer 18 (2018) 674.